New Dimensions in Colloidal Nanoparticle Characterization Enabled by Charge Detection

Mass Spectrometry

Conner C. Harper[†], Jacob S. Jordan[†], Steven Papanu[‡], and Evan R. Williams[†*]

†Department of Chemistry, University of California, Berkeley, California, 94720-1460, United States

‡2520 Wyandotte Street Suite F, Mountain View, CA, 94083-2381, United States

For submission to *ACS Nano*

[*]Address correspondence to this author.

Email: erw@berkeley.edu

Telephone: (510) 643-7161

Abstract

A variety of scattering-based, microscopy-based, and mobility-based methods are frequently used to probe the size distributions of colloidal nanoparticles with transmission electron microscopy (TEM) often considered to be the 'gold standard'. Charge detection mass spectrometry (CDMS) is an alternative method for nanoparticle characterization that can rapidly measure the mass and charge of individual nanoparticle ions with high accuracy. Two low polydispersity, ~100 nm diameter nanoparticle size standards with different compositions (polymethyl methacrylate/polystyrene co-polymer and 100% polystyrene) were characterized using both TEM and CDMS to explore the merits and complementary aspects of both methods. Mass and diameter distributions are rapidly obtained from CDMS measurements of thousands of individual ions of known spherical shape, requiring less time than TEM sample preparation and image analysis. TEM image-to-image variations resulted in a ~1-2 nm range in the determined mean diameters whereas the CDMS mass precision of ~1% in these experiments leads to a diameter uncertainty of just 0.3 nm. For the 100% polystyrene nanoparticles with known density, the CDMS and TEM particle diameter distributions were in excellent agreement. For the co-polymer nanoparticles with unknown density, the diameter from TEM measurements combined with the mass from CDMS measurements enabled an accurate measurement of nanoparticle density. Differing extents of charging for the two nanoparticle standards measured by CDMS show that charging is sensitive to nanoparticle surface properties. A mixture of the two samples were separated based on their different extents of charging despite having overlapping mass distributions centered at 341.5 and 331.0 MDa.

Introduction

Colloidal nanomaterials play an increasingly important role in a broad range of chemical

and biological applications. Methods that provide information about the size, shape, and surface

properties of nanomaterials are vital in understanding their synthesis pathways, chemistry, and

stability.[1–3] Several different methods are frequently used to characterize colloidal nanomaterials,

including dynamic light scattering (DLS), small-angle x-ray scattering (SAXS), scanning

electron microscopy (SEM), transmission electron microscopy (TEM), scanning tunneling

electron microscopy (STEM), atomic force microscopy (AFM), and differential mobility analysis

(DMA).[4–15] DLS and SAXS are ensemble measurements that use photon scattering from which

average nanomaterial properties are inferred.[4–7] These measurements have the advantage that

they are made directly from solution. In DMA analysis, nanoparticles must be ionized and

transferred into the gas phase where their mobilities, which are related to particle size and shape,

are measured.[12–15] As with DLS and SAXs, DMA analysis is also an ensemble-based

measurement, but unlike DLS and SAXS, DMA can separate and distinguish multiple

nanoparticle geometries and distinct size distributions present in a single sample with

uncertainties as low as ~1% of the nominal particle diameters.[14,15] Images provided by different

types of electron microscopies and AFM make it possible to obtain information about the

distribution of particle sizes and shapes from multiple individual particle measurements.[8–11]

Single particle methods are powerful tools to characterize nanoparticles, but challenges

associated with cost, sample preparation, and often labor-intensive image analysis can sometimes

preclude the use of these microscopy techniques in obtaining robust sampling statistics.

Nanoparticle standards that are traceable to National Institute of Standards and Technology (NIST) reference materials are used to calibrate various microscopy techniques and DMA. They are also used to validate DLS and SAXS measurements.[6,7] The relatively well-developed methodology for producing low polydispersity latex nanoparticles of controlled size and shape has led to their frequent use as standards, especially due to their relatively long-term colloidal stability, resistance to chemical modification, and low cost.[16] However, there can be significant variation (a few nanometers) in the mean measurements of these standards depending on which characterization technique is used.[8,9] Even with TEM, the most commonly used technique for nanoparticle characterization, the spread in the mean diameter measurement among different laboratories is around ~2 nm when directly measuring NIST reference materials.[11] Contributing factors to this variability include differences in focus, contrast, and image analysis methodologies. Thus, even when very low polydispersity standards are generated and analyzed using high precision methods, it can be difficult to accurately pinpoint the true mean diameter with a single measurement.[11]

Charge detection mass spectrometry (CDMS) is an alternative method to characterize synthetic nanoparticles that directly measures masses and charges of individual ionized nanoparticles[17–21] instead of inferring or imaging the physical dimensions such as the diameter. Mass is a fundamental property of molecules, molecular complexes, and nanoparticles, and the extent of charging in the electrospray ionization (ESI) process typically used to generate ions for CDMS analyses can provide information about shape and physical properties of the molecular surface.[22–27] In CDMS, similar to microscopy techniques, individual nanoparticle results are compiled into histograms to obtain the mass and charge distribution of a sample. CDMS is

distinct from conventional mass spectrometry methodologies where only mass-to-charge ratios (*m/z*) are measured for large ensembles of analytes that are typically <1 MDa. Previous work in CDMS has probed the masses of large nanoparticles and polymers[17–21,28–30] but the technique has only recently been applied directly to determining nanoparticle size distributions using new instrumentation with high resolution and high throughput.[18]

CDMS is well-suited to characterizing nanoparticles and nanoscale size standards with high precision. High mass accuracy can be obtained using known mass standards and/or by directly resolving charge states of individual ions with well-known masses.[31,32] If nanoparticle shape and density are well-defined, masses can then be directly translated to particle dimensions with very low error. For example, a mass precision of 1.5% translated to a diameter uncertainty of ~0.5% for ~100 nm spheres measured in previous work.[18] In contrast, there is relatively high variability inherent to calibrating image analysis methods, focus, and magnification in microscopy-based measurements.[8–11] Because the extent of nanoparticle charging is also measured in CDMS and should depend on surface properties, CDMS data can also potentially provide insights about nanoparticle shape and surface properties. In this work, ~100 nm latex nanoparticle standards produced by the Colloidal Metrics Corporation (hereafter referred to as CM nanoparticles) and by Thermo-Fisher Scientific (hereafter to referred by the product name, Nanospheres) were analyzed using both CDMS and TEM. The advantages and disadvantages of each technique and their complementary aspects are investigated in the context of these nanoparticle standards but are also more generally applicable to the characterization of all nanomaterials.

Comparing CDMS and TEM results. CDMS can analyze a large number of individual nanoparticles rapidly making it possible to obtain robust statistics and measure even subtle differences in nanoparticle distributions.[18] The masses of 2515 CM nanoparticles and 7072 Nanospheres were measured in ~16 and ~25 minutes, respectively, by CDMS and the resultant mass histograms are shown in Figure 1 with the CM nanoparticle data shown in blue and the Nanosphere data shown in red. For the CM nanoparticles, the main peak was fit with a Gaussian function with a mean of 341.5 MDa with a full width at half maximum (FWHM) of 30.5 MDa. Because of the negative skew of the Nanospheres distribution, the peak at 331.0 MDa and FWHM of 70.0 MDa were found by applying Savitzsky-Golay smoothing to the mass histogram and manually picking the peak maximum point and half-maximum points (bin size = 0.5 MDa). The narrower and more symmetrical mass distribution of the CM nanoparticles indicates lower polydispersity and greater size control in the synthesis of these nanoparticles. It is important to note that even the width of the mass range obtained for the more narrowly distributed CM nanoparticles reflects the heterogeneity in the sample and not a limitation in the mass accuracy of the CDMS instrument.[37] The few detected counts at lower mass (<100 MDa, <1% of total ion counts) for both nanoparticle types likely correspond to small impurities and/or small malformed nanoparticles.

To compare with and complement the CDMS data, TEM images were obtained for both the CM nanoparticles and Nanospheres and representative examples are shown in Figures 2A and 2B, respectively. Images were pre-processed and then analyzed by using an automated circle-fitting method based on the Hough circle transform.[18,36] The nanoparticle radii are returned by the method as integer numbers of pixels, which are then calibrated to diameters in

7

nanometers. An implicit assumption in this method to obtain diameters from the TEM data is that the nanoparticles are spherical, consistent with our observations for all of the particles that were fit. The pixel size of ~0.6 nm in these images was chosen as a compromise between magnification and keeping a statistically viable number of nanoparticles within the field of view of a single image and thereby reduce errors from combining measurements from large numbers of different image captures. Nanoparticles with poor edge contrast and/or apparent shape distortion as result of tight packing, such as the CM nanoparticles in the center of a hexagon-like arrangements in Figure 2A, have a poor fitting score in the circle-fitting method used here and are not detected or counted by this method. Exclusion of these poorly defined and/or apparently distorted nanoparticles is justified by the high quality of the circle fits of nanoparticles more clearly separated from their neighbors that indicate both nanoparticle types are highly spherical (more details are provided in the Supporting Information). More clearly separated nanoparticles are also more representative of their expected state in a relatively dilute colloidal suspension as opposed to the tight packing caused by drying process necessary for TEM imaging.

Slight differences in the magnification, background contrast, and/or focus also resulted in variable nanoparticle edge determination in image pre-processing. Because the automated analysis method relies on these edges to find appropriate circle fits and determine nanoparticle diameters, the peak of the diameter distribution in a single image varied by up to ~2 nm across multiple images. This variation between images was often greater than the width of the diameter distribution determined from a statistically significant number of nanoparticles within a single image, especially for the narrowly distributed CM nanoparticles. The mode of the diameter distribution for images containing >50 measured nanoparticles ranged from 92.8-94.9 nm for the

CM nanoparticles and from 98.6-100.2 nm for the Nanospheres, but the FWHM was consistent at ~3 nm for the CM nanoparticles and ~7 nm for the Nanospheres. High resolution DMA measurements obtained by de la Mora and co-workers for the same CM nanoparticles yielded an upper-bound for the mean diameter at ~100 nm and FWHM of 3%, consistent with these TEM results.[14] The higher mean diameter estimated by DMA may be due to retention of involatile solutes and unevaporated solvent in the ESI process used to generate gas-phase nanoparticles or due to uncertainties in the DMA calibration and flow rates.[14] The Nanospheres have a manufacturer certified, NIST-traceable mean diameter of 101 ± 3 nm which is also consistent with the observed range of TEM mean diameters.

In this work, the highest mean diameter measurements of 94.9 nm and 100.2 nm for the CM nanoparticles and Nanospheres, respectively, are used for further calculations. These measurements are taken to be most representative of the nanoparticles because the automated analysis method tended to increasingly underestimate the 'true' edges of the nanoparticles with decreasing contrast been the edges and the background. Examples of this phenomenon, along with more discussion about image-by-image variation, diameter measurements, and automated analysis method are provided in the Supporting Information. It is important to note that variations of ~1-2 nm in the mean of the diameter distribution of spherical nanoparticle standards measured among different TEM instruments[11] and among other microscopy methods[8,9] are common.

The representative diameter distributions shown in Figures 2C and 2D were generated from the 262 CM nanoparticles and 406 Nanospheres detected by the automated analysis in the images shown in Figures 2A and 2B, respectively. These distributions obtained from single TEM

9

images are generally consistent with the CDMS mass data where the CM nanoparticles have a narrower, more symmetrical distribution of size whereas the Nanospheres have a broader distribution that skews toward smaller sizes. The CM nanoparticles have smaller diameters but higher masses than the Nanospheres, indicating that the CM nanoparticles must be significantly denser. This observation is also supported by the darker contrast of the CM nanoparticles relative to the Nanospheres in the TEM images (Figures 2A and 2B). The density of the Nanospheres is expected to be very close to the 1.0502 g/mL bulk value for polystyrene[38] based on their 100% polystyrene composition as well as density measurements of similar polystyrene nanoparticles using analytical ultracentrifugation techniques.[39] The bulk density of the co-polymer used in the CM nanoparticle synthesis and the density of the CM nanoparticles themselves have not previously been measured. However, one way of estimating the density of the CM nanoparticles is to use a weighted average of the bulk component polymer densities (86% polystyrene at 1.0502 g/mL,[38] 14% PMMA at 1.185 g/mL[40]), which yields a value of 1.069 g/mL.

Nanoparticle Density Determination by CDMS and TEM. For spherical particles, CDMS mass distributions can be directly transformed into diameter distributions if the density of the material is known. Figure 3a shows the diameter distributions determined for the CM nanoparticles (blue) and the Nanospheres (red) by CDMS using the density estimates based on their respective bulk values detailed above. The Nanospheres peak diameter determined by CDMS is 100.0 nm and is within the range determined by the TEM images (98.6-100.2 nm). It approaches the upper edge of the range determined from TEM images, which is also consistent a slight underestimation in TEM diameters by the automated analysis. In contrast, the peak diameter for the CM nanoparticles determined by CDMS from the estimated density is 100.4 nm,

a value that is significantly higher than the diameters obtained from the TEM measurements (92.8-94.9 nm).

For nanoparticles where the density is unknown and/or potentially inconsistent with predictions based on bulk values, a combination of CDMS peak masses and TEM peak diameters can be used to directly determine density. Assuming a perfectly spherical geometry, average densities of 1.265 g/mL and 1.045 g/mL were determined using the CDMS peak masses and the TEM peak diameters for the CM nanoparticles and Nanospheres, respectively. The measured Nanosphere density is nearly a perfect match with the density of bulk polystyrene (1.0502 g/mL), consistent with the pure polystyrene composition of these nanoparticles. This match between the measured density of the Nanospheres and bulk polystyrene demonstrates that complementary CDMS and TEM analyses can determine nanoparticle densities with high accuracy similar to that achieved using analytical ultracentrifugation techniques.[39] However, the measured density of 1.265 g/mL for the co-polymer-based CM nanoparticles is significantly higher than the value estimated from the average of the bulk constituents used in the synthesis. There are a few possible explanations for this observation. The first and most likely explanation is that the CM nanoparticles undergo some shrinkage due to the electron beam of the TEM as a result of inclusion of PMMA as a co-polymer. Shrinkage/degradation of organic polymer-based nanoparticles and thin films under irradiation by an electron beam is well-documented.[41–44] PMMA is used as both a positive and negative electron beam resist in nanolithography,[43,44] indicating that some degradation of the PMMA in these nanospheres may also occur. It is also possible that the inclusion of the PMMA as a co-polymer results in a denser packing structure than either of the pure individual constituent polymers. The CDMS mass measurements also

could be high because surfactants used as part of the nanoparticle synthesis adduct to the nanoparticles and are included in the mass measured by CDMS due to the relatively 'soft' nature of ESI but are removed during the harsher sample drying process in preparation for TEM analysis.

Once nanoparticle densities and shape are known, nanoparticle diameters can be directly determined from CDMS data. Figure 3B shows the diameter distributions of CM nanoparticles (blue) and Nanospheres (red) obtained from the measured CDMS masses using the directly determined densities for the CM nanoparticles and Nanospheres of 1.265 g/mL and 1.045 g/mL, respectively. The CM nanoparticle diameter distribution peak is 94.9 nm with a FWHM of 2.9 nm whereas the Nanospheres peak is 100.2 nm with a FWHM of 7.2 nm. In addition to the expected match of diameter peaks between CDMS and TEM because the densities used are based on the CDMS masses and TEM diameters, the widths and overall shape of the diameter distributions also match very closely, indicating that both nanoparticle types have a relatively homogeneous distribution of densities (i.e. a single value for the density can be reasonably applied to all the observed nanoparticles of a given type). For nanoparticles with a broad distribution of densities (e.g. porous materials), a density distribution could be estimated using the differences in peak width and shape between the TEM and CDMS diameter distributions.

There are distinctive advantages associated with determining diameters directly from CDMS data. The much higher counts of individual nanoparticle measurements obtainable by CDMS in a relatively short period come without the challenges associated with image-to-image variation and make it possible to gain a clearer statistical picture of nanoparticle populations. The precision of the diameter determination using CDMS is also equal to or greater than TEM even

while operating at the high data acquisition rate used here. For the ~100 nm nanoparticle standards measured in this work, a short 100 ms trapping period was used and the uncertainty in the mass measurement of any given nanoparticle is ~1%, varying slightly depending on the charge state and ion energy. Because mass is proportional to the cube of the diameter, the uncertainty in the diameter of each individual nanoparticle is only ~0.3% (~0.3 nm) in the CDMS analysis using a spherical model. When longer trapping periods are used, CDMS mass uncertainties as low as ~0.1% can be achieved for nanoparticles of similar size and charge to those analyzed in this work,[20] which translates to sub-angstrom (~0.03 nm) diameter precision. In practice, this level of precision is not likely to be useful because it represents a length scale shorter than the shortest chemical bond. Nevertheless, this demonstrates the advantages of using the relatively high precision masses determined by CDMS to characterize the diameter or other relevant dimensions of nanoparticles with a known shape and density.

Charge Measurement in CDMS is Sensitive to Surface Properties. In addition to mass and diameter characterization, CDMS also provides independent measurements of the charge deposited on each individual nanoparticle in the ESI process. For biomolecules such as proteins, protein complexes, and even small viruses, the extent of charging in ESI is related to the surface area exposed to solution during the ESI process.[22–27] For approximately spherical analytes, this extent of charging should then also be related to the analyte diameter. However, the two-dimensional histograms of mass vs. charge for both CM nanoparticles (Fig. 4A) and Nanospheres (Fig. 4B), show that even at comparable masses, charging is significantly greater for the CM nanoparticles. The CM nanoparticles have a peak charge of 949 e at the peak mass of 341.5 MDa, and the Nanospheres have a peak charge of 772 e at the peak mass of 331.0 MDa.

13

The Nanospheres have an overall larger spread of charging, but this is primarily due to the broader mass distribution; the width of the charging distribution at a single mass value (i.e., a vertical line in the two-dimensional histograms of Figure 4) is similar between the two samples. The dashed blue line indicates the Rayleigh charge limit for an aqueous droplet of corresponding mass.[45] Globular analytes with heteroatoms, such as proteins, DNA, RNA, etc. typically charge near or slightly below the Rayleigh limit.[27,46,47] Despite being generated from aqueous dispersions, both nanoparticle types have charge distributions well below the Rayleigh limit. The higher/different densities of these nanoparticles relative to water contribute to this apparent effect, but even when using the Rayleigh charge limit determined directly from the TEM diameters instead of the mass, the CM nanoparticles and Nanospheres are only charged to 73% and 55% of the Rayleigh limit, respectively. These values are below those observed for extensive heteroatom-containing compounds, such as proteins and protein complexes, which typically have average charge states at ~80% of the Rayleigh limit.[27,46,47]

The overall charge of these spherical nanoparticles depends not only on the available surface area, but also on the surface properties of the particles. Nanospheres are composed of ~100% polystyrene, which does not contain any functional groups with high gas-phase basicity that are typically considered as the most likely hosts for protons or other cations in the final stages of desolvation in the ESI process.[48,49] The high gas-phase basicity of globular proteins results in the retention of protons from water molecules and clusters that evaporate from the droplet surface,[50–53] leading to charge states that are close to the Rayleigh charging limit for a water droplet of similar size to the analyte.[27,54,55] The PMMA co-polymer included in the CM nanoparticles contains an ester group that is an obvious candidate for protonation or salt ion

14

adduction. Coordination of either a proton or a salt ion by two or more oxygen atoms will increase the ability of these particles to retain charge compared to the 100% polystyrene nanospheres that consists of just carbon and hydrogen and where multi-site coordination is not likely. The lower basicity of the polystyrene makes it more energetically favorable for water clusters to carry away protons or other cations until the apparent gas-phase basicity or ion binding energy of the particle increases above that of water or water clusters due to lower Coulombic repulsion. This would lead to the lower charge states observed for the 100% polystyrene nanospheres. This ability of CDMS to rapidly probe chemical composition is a valuable addition to making accurate mass measurements on a nanoparticle-by-nanoparticle basis. While nanoparticle surface properties could potentially be characterized more specifically by other methods, the broad scope, rapid acquisition, and lack of additional experimental burden associated with CDMS analysis is an important advantage, especially in applications such as quality control in nanoparticle synthesis.

The different extents of charging for the CM nanoparticles and Nanospheres in Figure 4 can be affected by inconsistencies or subtle differences in the ESI process for each sample. It is worth noting that in previous CDMS measurements of the same Nanospheres standard using the same instrument that was used here, the peak mass was higher (354 MDa) and the average charge was much higher (~1200 e) with a broader distribution that was closer to the Rayleigh limit (~85%).[18] The difference between these prior measurements and the current work almost certainly originates from incomplete desolvation in the initial Nanospheres measurements, where the still hydrated surface of the nanoparticle caused both the higher mass and charging. As a result, the estimated peak diameter for the Nanospheres was also ~3 nm higher than diameters

determined by TEM image analysis in the previous work,[18] whereas in the current work, the density calculated using the combination of TEM diameters and CDMS masses yielded a nearly perfect match to the bulk density expected for 100% polystyrene particles. The close agreement between the bulk and measured density for the 100% polystyrene Nanospheres and the narrower charge distributions characteristic of dry analytes indicate that a much-improved extent of desolvation was achieved here for both the Nanospheres and the CM nanoparticles.

Despite gaining improved knowledge about how to better desolvate MDa size analytes, ESI variability still can lead to slightly different extents of solvation. A straightforward method to compare nanoparticle surface properties is to mix dispersions of CM nanoparticles and Nanospheres in equal concentration and analyze the mixture by CDMS. The resultant two-dimensional histogram is shown in Figure 5 and is composed of 4007 ions acquired in ~30 minutes. The distribution of CM nanoparticles at higher charge and mass is readily distinguishable from the Nanospheres distribution, which is identifiable from its characteristic tailing to lower mass and charge. The peak masses and charges of the two distributions are ~347 MDa and ~336 MDa and ~1075 e and ~865 e, for the CM nanoparticles and Nanospheres, respectively. The mass peaks for both standards are ~1.5% greater than those of the separate measurements shown in Figure 4 and the charge peaks are both ~12% higher. The slightly increased mass and much larger increase in charge indicates that the nanoparticles likely retained a small amount of solvent from the ESI process in this experiment. It is worth noting that despite this solvent retention, diameters determined from these data are robust to mass shifts and change by only ~0.5% due to the favorable cubic scaling between mass and diameter.

Despite these differences from the separate observations in Figure 4, it is clear that the CM nanoparticles have a propensity to charge higher than the Nanospheres. These data also show that water can charge more readily than either of the dry nanoparticle surfaces, an observation consistent with recent charging measurements of ~100 nm aqueous nanodroplets that were at or even above the Rayleigh charging limit (blue dashed line in Figures 4 and 5). Thus, under more solvated conditions, it is likely that the two nanoparticle charging distributions would begin to merge at values close to the Rayleigh limit, but this is the expected behavior for a technique sensitive to surface composition as the surface itself starts to resemble a solvent droplet. Conditions to produce "drier" nanoparticle ions are important to understand and are a subject of continued study; the desolvation process for MDa-size analytes generated from ESI of aqueous solutions is not yet well understood.

Conclusions

CDMS is an important addition to the analytical toolbox used to study nanomaterials. Mass is a fundamental property of matter and is often closely related to the properties of nanomaterials. If the shape and density are known, the masses of completely desolvated nanoparticles can also be translated into the physical dimensions of the nanoparticles with very high precision. Further work to understand variation in ESI conditions and the desolvation process for large macromolecules such as nanoparticles will help to ensure that ions are fully desolvated. In cases where the density and/or the shape are unknown, CDMS is complemented well by imaging techniques, such as TEM, that can determine the shape and physical dimensions of individual particles to provide a model for the conversion of measured nanoparticle masses to nanoparticle dimensions. The combination of these techniques can make it possible to determine

17

the density of nanoparticles *ab initio*, removing the need for bulk approximations that can be erroneous. Density measurements of this type could have many useful applications in characterizing porous nanoparticles, nanocapsules, and other types of nanomaterials where the density may vary from that of the bulk components.

In addition to the information provided by the mass measurement alone, CDMS also provides a measurement of charge that can give further insight into nanoparticle shape and surface composition. A large number of nanomaterials rely on some type of surface functionalization in their various applications. The ability of CDMS to resolve subtle differences between nanoparticle standards demonstrated in this work is not only important for techniques that rely on these standards for calibration but also for the general characterization of nanomaterials. The ability to determine mass distributions and differentiate between surface compositions, combined with the high speed of CDMS analysis, makes CDMS a powerful technique for quality control in both research and industrial scale nanomaterial synthesis.

Experimental

Materials. A sample of Nanospheres size standard polystyrene spheres (1% w/v in aqueous suspension) with a calibrated mean diameter of 101 ± 3 nm and a standard deviation of 6.2 nm was obtained from Thermo Scientific (catalog no. 3100/3100A) and diluted by a factor of 200 into 0.5% aqueous acetic acid. The calibrated mean diameter of 101 ± 3 nm (certified batch no. 3100-009) is certified by the manufacturer via transfer by TEM from NIST reference materials. A sample of ~100 nm CM nanoparticles was obtained from Professor Juan Fernandez de la Mora at Yale University who obtained them from Colloidal Metrics. The ~100 nm CM nanoparticle sample was synthesized with ~0.64% w/v of co-polymer (86% polystyrene and 14%

polymethyl methacrylate by mass) solids and ~0.15% non-polymer solids in an aqueous suspension and were diluted by a factor of 150 into 0.5% aqueous acetic acid. A mixture of CM nanoparticles and Nanospheres was made by mixing the diluted samples of each type in equal volume.

Charge Detection Mass Spectrometry. A custom-built CDMS instrument was used for all mass spectrometry experiments and has been described in detail elsewhere.[18] Briefly, ions were generated using nanoelectrospray ionization from borosilicate emitters with tip diameters of 3-5 μm. Ions pass through a heated drying capillary and multiple stages of ion optics and differential pumping until reaching an electrostatic conetrap where they are trapped for 100 ms. During the trapping period, ions repeatedly pass through a conductive cylinder in the center of the trap and induce periodic current pulses with amplitudes proportional to the ion charge. The signal is amplified by a charge-sensitive preamplifier and subsequent bandpass filter stage before it is digitized at 1 MHz. Signals are analyzed using a program that performs unapodized short-time Fourier transforms (STFT), picks and fits the fundamental and multiple harmonic frequency peaks for each ion signal in each STFT segment and uses the resultant centroid frequencies and amplitudes to dynamically determine the mass, charge, and energy of each ion throughout the entire trapping period.[20,32,33] Multiple ions are routinely trapped and analyzed simultaneously;[34,35] frequency overlap events that resulted in ions being discarded made up <1% of all ion signals. The mass resolution of the CDMS used in this work depends on the charge states of the analytes and the length of the trapping period, which establishes the measurement time. For the 100 ms trapping periods and ions with ~800 charges, the mass uncertainty is ~1%, or, in other words, a mass resolution of ~100. The relatively broad mass distributions of nanoparticles mean that mass

spectral peak widths are entirely controlled by sample heterogeneity and not by instrument resolution. CDMS mass measurements were calibrated using macromolecules of known mass in the ~500 kDa – 10 MDa range. This lower calibrant mass range is necessary because analytes that are sufficiently homogeneous to serve as mass standards do not exist in the 100+ MDa size range.

Transmission Electron Microscopy. Prior to TEM analysis, both samples were diluted in pure water by a factor of ∼40. Formvar/carbon-coated 300 mesh copper grids (Ted Pella Inc.) were made hydrophilic with an easiGlow (Pelco) benchtop glow discharge unit. A 5 µL volume of sample was placed on each grid for 5 min before being manually dried using clean filter paper. Sample-coated grids were imaged using a Tecnai 12 120 kV transmission electron microscope (FEI). Images were recorded using a Rio 16 CMOS with DigitalMicrograph software (Gatan Inc.). The TEM magnification selected for these experiments resulted in resolution of ∼0.6 nm/pixel. The resulting TEM images were analyzed using FIJI/ImageJ version 1.53v. An automated analysis method based on the Hough Circle Transform was used to find circle fit radii and has been described in detail elsewhere.[18,36] Diameter distributions were generated for each individual image due to image-to-image variations in the measurements (more details in the Supporting Information).

Acknowledgements

at the University of California, Berkeley Electron Microscope Laboratory, for advice and assistance in TEM image collection.

Supporting Information

Additional TEM experimental details including TEM images, corresponding size distributions, and overlaid automated analysis circle fits.

Conflicts of Interest. Steven Papanu is the president of Colloidal Metrics Corporation who supplied one of the samples used in this work and contributed insights into the composition and synthesis of nanoparticles. All measurements and analysis of both CDMS and TEM data were performed at UC Berkeley and all of the other coauthors have no conflicts of interest.

References

(1) Baek, W.; Chang, H.; Bootharaju, M. S.; Kim, J. H.; Park, S.; Hyeon, T. Recent Advances and Prospects in Colloidal Nanomaterials. *JACS Au* **2021**, *1* (11), 1849–1859.

(2) Mourdikoudis, S.; Pallares, R. M.; Thanh, N. T. K. Characterization Techniques for Nanoparticles: Comparison and Complementarity upon Studying Nanoparticle Properties. *Nanoscale* **2018**, *10* (27), 12871–12934.

(3) Ealias, A. M.; Saravanakumar, M. P. A Review on the Classification, Characterisation, Synthesis of Nanoparticles and Their Application. *IOP Conf. Ser. Mater. Sci. Eng.* **2017**, *263* (3), 32019.

(4) Ramos, A. P. Dynamic Light Scattering Applied to Nanoparticle Characterization. In *Nanocharacterization Techniques*; William Andrew Publishing, 2017; pp 99–110.

(5) Li, T.; Senesi, A. J.; Lee, B. Small Angle X-Ray Scattering for Nanoparticle Research. *Chem. Rev.* **2016**, *116* (18), 11128–11180.

(6) Takahashi, K.; Kato, H.; Saito, T.; Matsuyama, S.; Kinugasa, S. Precise Measurement of the Size of Nanoparticles by Dynamic Light Scattering with Uncertainty Analysis. *Part. Part. Syst. Charact.* **2008**, *25* (1), 31–38.

(7) Kuzmanovic, D. A.; Elashvili, I.; O'Connell, C.; Krueger, S. A Novel Application of Small-Angle Scattering Techniques: Quality Assurance Testing of Virus Quantification Technology. *Radiat. Phys. Chem.* **2008**, *77* (3), 215–224.

(8)   Teulon, J. M.; Godon, C.; Chantalat, L.; Moriscot, C.; Cambedouzou, J.; Odorico, M.; Ravaux, J.; Podor, R.; Gerdil, A.; Habert, A.; Herlin-Boime, N.; Chen, S. W. W.; Pellequer, J. L. On the Operational Aspects of Measuring Nanoparticle Sizes. *Nanomaterials* **2019**, *9* (1), 18.

(9)   Tuoriniemi, J.; Johnsson, A. C. J. H.; Holmberg, J. P.; Gustafsson, S.; Gallego-Urrea, J. A.; Olsson, E.; Pettersson, J. B. C.; Hassellöv, M. Intermethod Comparison of the Particle Size Distributions of Colloidal Silica Nanoparticles. *Sci. Technol. Adv. Mater.* **2014**, *15* (3), 35009.

(10)   Borchert, H.; Shevchenko, E. V.; Robert, A.; Mekis, I.; Kornowski, A.; Grübel, G.; Weller, H. Determination of Nanocrystal Sizes: A Comparison of TEM, SAXS, and XRD Studies of Highly Monodisperse CoPt 3 Particles. *Langmuir* **2005**, *21* (5), 1931–1936.

(11)   Rice, S. B.; Chan, C.; Brown, S. C.; Eschbach, P.; Han, L.; Ensor, D. S.; Stefaniak, A. B.; Bonevich, J.; Vladár, A. E.; Walker, A. R. H.; Zheng, J.; Starnes, C.; Stromberg, A.; Ye, J.; Grulke, E. A. Particle Size Distributions by Transmission Electron Microscopy: An Interlaboratory Comparison Case Study. *Metrologia* **2013**, *50* (6), 663–678.

(12)   Li, C.; Lee, A. L.; Chen, X.; Pomerantz, W. C. K.; Haynes, C. L.; Hogan, C. J. Multidimensional Nanoparticle Characterization through Ion Mobility-Mass Spectrometry. *Anal. Chem.* **2020**, *92* (3), 2503–2510.

(13)   Tan, J.; Liu, J.; Li, M.; El Hadri, H.; Hackley, V. A.; Zachariah, M. R. Electrospray-Differential Mobility Hyphenated with Single Particle Inductively Coupled Plasma Mass Spectrometry for Characterization of Nanoparticles and Their Aggregates. *Anal. Chem.* **2016**, *88* (17), 8548–8555.

(14)   Fernandez de la Mora, J.; Kramar, J.; Farkas, N.; Papanu, S.; Dana, R. Singularly Narrow Size Distributions of 200 Nm Polystyrene Latex Spheres Determined by High Resolution Mobility Analysis. *J. Aerosol Sci.* **2023**, *170*, 106158.

(15)   Fernandez de la Mora, J.; Papanu, S. Technical Note: Characterization of Polystyrene Latex Spheres 300 Nm in Diameter with a Singularly Narrow Size Distribution. *J. Aerosol Sci.* **2023**, *173*, 106230.

(16)   Rao, J. P.; Geckeler, K. E. Polymer Nanoparticles: Preparation Techniques and Size-Control Parameters. *Prog. Polym. Sci.* **2011**, *36* (7), 887–913.

(17)   Elliott, A. G.; Merenbloom, S. I.; Chakrabarty, S.; Williams, E. R. Single Particle Analyzer of Mass: A Charge Detection Mass Spectrometer with a Multi-Detector Electrostatic Ion Trap. *Int. J. Mass Spectrom.* **2017**, *414*, 45–55.

(18)   Harper, C. C.; Miller, Z. M.; McPartlan, M. S.; Jordan, J. S.; Pedder, R. E.; Williams, E. R. Accurate Sizing of Nanoparticles Using a High-Throughput Charge Detection Mass Spectrometer without Energy Selection. *ACS Nano* **2023**, *17* (8), 7765–7774.

(19)   Harper, C. C.; Avadhani, V. S.; Hanozin, E.; Miller, Z. M.; Williams, E. R. Dynamic Energy Measurements in Charge Detection Mass Spectrometry Eliminate Adverse Effects

of Ion–Ion Interactions. *Anal. Chem.* **2023**, *95* (26), 10077–10086.

(20)   Harper, C. C.; Miller, Z. M.; Williams, E. R. Combined Multiharmonic Frequency Analysis for Improved Dynamic Energy Measurements and Accuracy in Charge Detection Mass Spectrometry. *Anal. Chem.* **2023**, *95* (45), 16659–16667.

(21)   Doussineau, T.; Santacreu, M.; Antoine, R.; Dugourd, P.; Zhang, W.; Chaduc, I.; Lansalot, M.; D'Agosto, F.; Charleux, B. The Charging of Micellar Nanoparticles in Electrospray Ionization. *ChemPhysChem* **2013**, *14* (3), 603–609.

(22)   Fenn, J. B.; Mann, M.; Meng, C. K.; Wong, S. F.; Whitehouse, C. M. Electrospray Ionization–Principles and Practice. *Mass Spectrom. Rev.* **1990**, *9* (1), 37–70.

(23)   Barnes, L. F.; Draper, B. E.; Jarrold, M. F. Analysis of Recombinant Adenovirus Vectors by Ion Trap Charge Detection Mass Spectrometry: Accurate Molecular Weight Measurements beyond 150 MDa. *Anal. Chem.* **2022**, *94* (3), 1543–1551.

(24)   Harper, C. C.; Brauer, D. D.; Francis, M. B.; Williams, E. R. Direct Observation of Ion Emission from Charged Aqueous Nanodrops: Effects on Gaseous Macromolecular Charging. *Chem. Sci.* **2021**, *12* (14), 5185–5195.

(25)   Hanozin, E.; Harper, C. C.; McPartlan, M. S.; Williams, E. R. Dynamics of Rayleigh Fission Processes in ∼100 Nm Charged Aqueous Nanodrops. *ACS Cent. Sci.* **2023**, *9* (8), 1611–1622.

(26)   Chowdhury, S. K.; Katta, V.; Chait, B. T. Probing Conformational Changes in Proteins by Mass Spectrometry. *J. Am. Chem. Soc.* **1990**, *112* (24), 9012–9013.

(27)   Fernandez De La Mora, J. Electrospray Ionization of Large Multiply Charged Species Proceeds via Dole's Charged Residue Mechanism. *Anal. Chim. Acta* **2000**, *406* (1), 93–104.

(28)   Antoine, R.; Doussineau, T.; Dugourd, P.; Calvo, F. Multiphoton Dissociation of Macromolecular Ions at the Single-Molecule Level. *Phys. Rev. A - At. Mol. Opt. Phys.* **2013**, *87* (1), 013435.

(29)   Doussineau, T.; Bao, C. Y.; Antoine, R.; Dugourd, P.; Zhang, W.; D'Agosto, F.; Charleux, B. Direct Molar Mass Determination of Self-Assembled Amphiphilic Block Copolymer Nanoobjects Using Electrospray-Charge Detection Mass Spectrometry. *ACS Macro Lett.* **2012**, *1* (3), 414–417.

(30)   Elliott, A. G.; Harper, C. C.; Lin, H. W.; Williams, E. R. Mass, Mobility and MS[N] Measurements of Single Ions Using Charge Detection Mass Spectrometry. *Analyst* **2017**, *142* (15), 2760–2769.

(31)   Todd, A. R.; Jarrold, M. F. Dynamic Calibration Enables High-Accuracy Charge Measurements on Individual Ions for Charge Detection Mass Spectrometry. *J. Am. Soc. Mass Spectrom.* **2020**, *31* (6), 1241–1248.

(32)   Miller, Z. M.; Harper, C. C.; Lee, H.; Bischoff, A. J.; Francis, M. B.; Schaffer, D. V.;

Williams, E. R. Apodization Specific Fitting for Improved Resolution, Charge Measurement, and Data Analysis Speed in Charge Detection Mass Spectrometry. *J. Am. Soc. Mass Spectrom.* **2022**, *33* (11), 2129–2137.

(33)   Harper, C. C.; Elliott, A. G.; Lin, H. W.; Williams, E. R. Determining Energies and Cross Sections of Individual Ions Using Higher-Order Harmonics in Fourier Transform Charge Detection Mass Spectrometry (FT-CDMS). *J. Am. Soc. Mass Spectrom.* **2018**, *29* (9), 1861–1869.

(34)   Harper, C. C.; Elliott, A. G.; Oltrogge, L. M.; Savage, D. F.; Williams, E. R. Multiplexed Charge Detection Mass Spectrometry for High-Throughput Single Ion Analysis of Large Molecules. *Anal. Chem.* **2019**, *91* (11), 7458–7468.

(35)   Harper, C. C.; Williams, E. R. Enhanced Multiplexing in Fourier Transform Charge Detection Mass Spectrometry by Decoupling Ion Frequency from Mass to Charge Ratio. *J. Am. Soc. Mass Spectrom.* **2019**, *30* (12), 2637–2645.

(36)   Mirzaei, M.; Rafsanjani, H. K. An Automatic Algorithm for Determination of the Nanoparticles from TEM Images Using Circular Hough Transform. *Micron* **2017**, *96*, 86–95.

(37)   Harper, C. C.; Miller, Z. M.; Lee, H.; Bischoff, A. J.; Francis, M. B.; Schaffer, D. V.; Williams, E. R. Effects of Molecular Size on Resolution in Charge Detection Mass Spectrometry. *Anal. Chem.* **2022**, *94* (33), 11703–11712.

(38)   Godin, M.; Bryan, A. K.; Burg, T. P.; Babcock, K.; Manalis, S. R. Measuring the Mass, Density, and Size of Particles and Cells Using a Suspended Microchannel Resonator. *Appl. Phys. Lett.* **2007**, *91* (12), 123121.

(39)   Minelli, C.; Sikora, A.; Garcia-Diez, R.; Sparnacci, K.; Gollwitzer, C.; Krumrey, M.; Shard, A. G. Measuring the Size and Density of Nanoparticles by Centrifugal Sedimentation and Flotation. *Anal. Methods* **2018**, *10* (15), 1725–1732.

(40)   Goseki, R.; Ishizone, T. Poly(Methyl Methacrylate) (PMMA) BT - Encyclopedia of Polymeric Nanomaterials; Kobayashi, S., Müllen, K., Eds.; Springer Berlin Heidelberg: Berlin, Heidelberg, 2015; pp 1702–1710.

(41)   Jung, K. Y.; Park, B. C.; Song, W. Y.; O, B. H.; Eom, T. B. Measurement of 100-Nm Polystyrene Sphere by Transmission Electron Microscope. *Powder Technol.* **2002**, *126* (3), 255–265.

(42)   Mulholland, G. W.; Duelge, K. J.; Hackley, V. A.; Farkas, N.; Kramar, J. A.; Zachariah, M. R.; Takahata, K.; Sakurai, H.; Ehara, K. Measurement of 100 Nm Monodisperse Particles by Four Accurate Methods: Traceability and Uncertainty. *Aerosol Sci. Technol.* **2024**, *58* (3), 323–333.

(43)   Yasuda, M.; Furukawa, Y.; Kawata, H.; Hirai, Y. Multiscale Simulation of Resist Pattern Shrinkage during Scanning Electron Microscope Observations. *J. Vac. Sci. Technol. B, Nanotechnol. Microelectron. Mater. Process. Meas. Phenom.* **2015**, *33* (6), 06FH02.

(44) Gautsch, S.; Studer, M.; de Rooij, N. F. Complex Nanostructures in PMMA Made by a Single Process Step Using E-Beam Lithography. *Microelectron. Eng.* **2010**, *87* (5–8), 1139–1142.

(45) Rayleigh, Lord. XX. On the Equilibrium of Liquid Conducting Masses Charged with Electricity. *London, Edinburgh, Dublin Philos. Mag. J. Sci.* **1882**, *14* (87), 184–186.

(46) Heck, A. J. R.; Van Den Heuvel, R. H. H. Investigation of Intact Protein Complexes by Mass Spectrometry. *Mass Spectrom. Rev.* **2004**, *23* (5), 368–389.

(47) Susa, A. C.; Xia, Z.; Tang, H. Y. H.; Tainer, J. A.; Williams, E. R. Charging of Proteins in Native Mass Spectrometry. *J. Am. Soc. Mass Spectrom.* **2017**, *28* (2), 332–340.

(48) Oss, M.; Kruve, A.; Herodes, K.; Leito, I. Electrospray Ionization Efficiency Scale of Organic Compound. *Anal. Chem.* **2010**, *82* (7), 2865–2872.

(49) Banerjee, S.; Mazumdar, S. Electrospray Ionization Mass Spectrometry: A Technique to Access the Information beyond the Molecular Weight of the Analyte. *Int. J. Anal. Chem.* **2012**, *2012*, 1–40.

(50) Gross, D. S.; Schnier, P. D.; Rodriguez-Cruz, S. E.; Fagerquist, C. K.; Williams, E. R. Conformations and Folding of Lysozyme Ions in Vacuo. *Proc. Natl. Acad. Sci. U. S. A.* **1996**, *93* (7), 3143–3148.

(51) Williams, E. R. Proton Transfer Reactivity of Large Multiply Charged Ions. *J. Mass Spectrom.* **1996**, *31* (8), 831–842.

(52) Rodriguez-Cruz, S. E.; Klassen, J. S.; Williams, E. R. Hydration of Gas-Phase Gramicidin S (M + 2H)2+ Ions Formed by Electrospray: The Transition from Solution to Gas-Phase Structure. *J. Am. Soc. Mass Spectrom.* **1997**, *8* (5), 565–568.

(53) Rodriguez-Cruz, S. E.; Klassen, J. S.; Williams, E. R. Hydration of Gas-Phase Ions Formed by Electrospray Ionization. *J. Am. Soc. Mass Spectrom.* **1999**, *10* (10), 958–968.

(54) Iavarone, A. T.; Williams, E. R. Mechanism of Charging and Supercharging Molecules in Electrospray Ionization. *J. Am. Chem. Soc.* **2003**, *125* (8), 2319–2327.

(55) Abramsson, M. L.; Sahin, C.; Hopper, J. T. S.; Branca, R. M. M.; Danielsson, J.; Xu, M.; Chandler, S. A.; Österlund, N.; Ilag, L. L.; Leppert, A.; Costeira-Paulo, J.; Lang, L.; Teilum, K.; Laganowsky, A.; Benesch, J. L. P.; Oliveberg, M.; Robinson, C. V.; Marklund, E. G.; Allison, T. M.; Winther, J. R.; Landreh, M. Charge Engineering Reveals the Roles of Ionizable Side Chains in Electrospray Ionization Mass Spectrometry. *JACS Au* **2021**, *1* (12), 2385–2393.
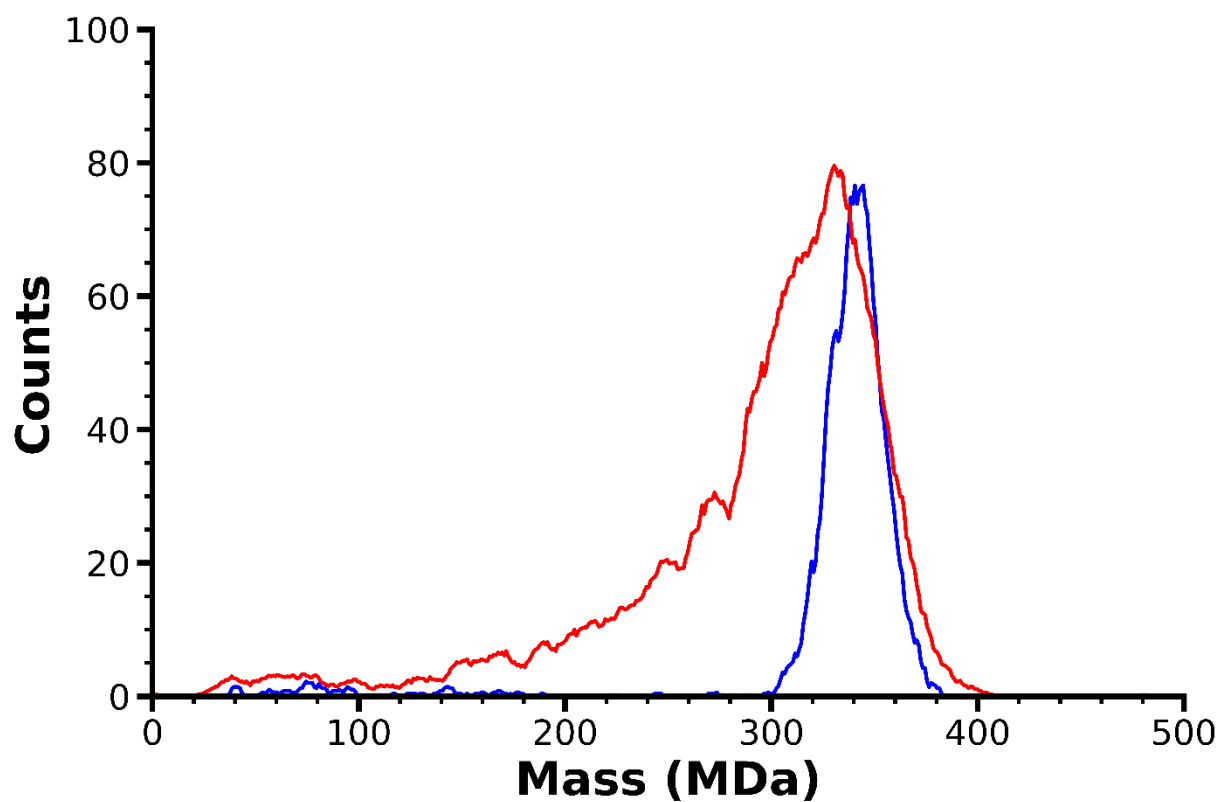
Figures

Figure 1. Mass histograms from CDMS measurements of 2515 CM nanoparticles (blue) and

7072 Nanospheres (red) with peak masses at 341.5 MDa and 331.0 MDa, respectively. The CM

particles exhibit a much narrower and more symmetrical distribution indicative of a more low
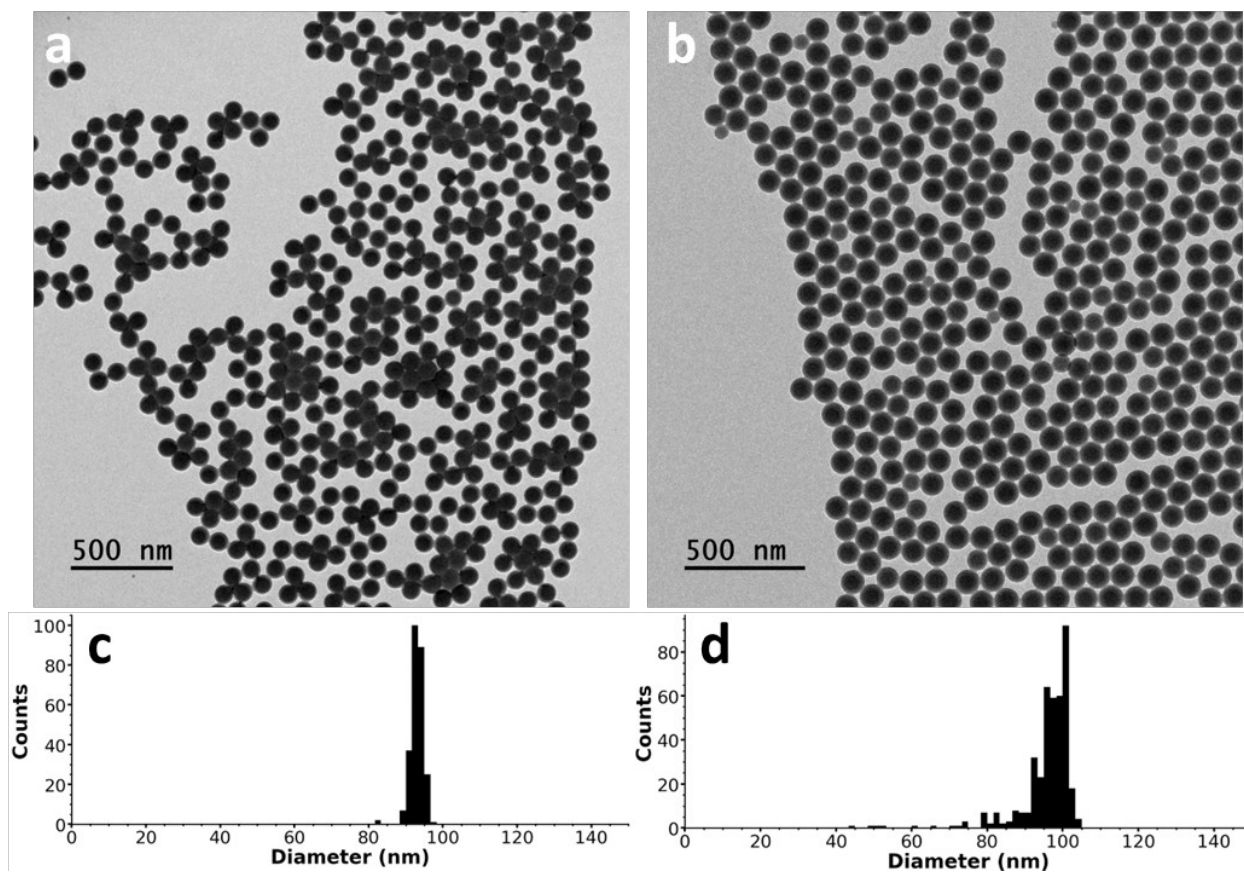
polydispersity sample.

Figure 2. Representative TEM images and corresponding diameter distributions determined by automated analysis of single images of both the CM nanoparticles (a, c) and Nanospheres (b, d). Some tightly packed clusters of CM nanoparticles in (a) resulted in poor edge contrast that precluded automated analysis resulting in fewer total counts (262) compared to the Nanospheres (406). More TEM images and examples of image-to-image variation in the diameter distributions of these both nanoparticle types are included in the Supporting Information.
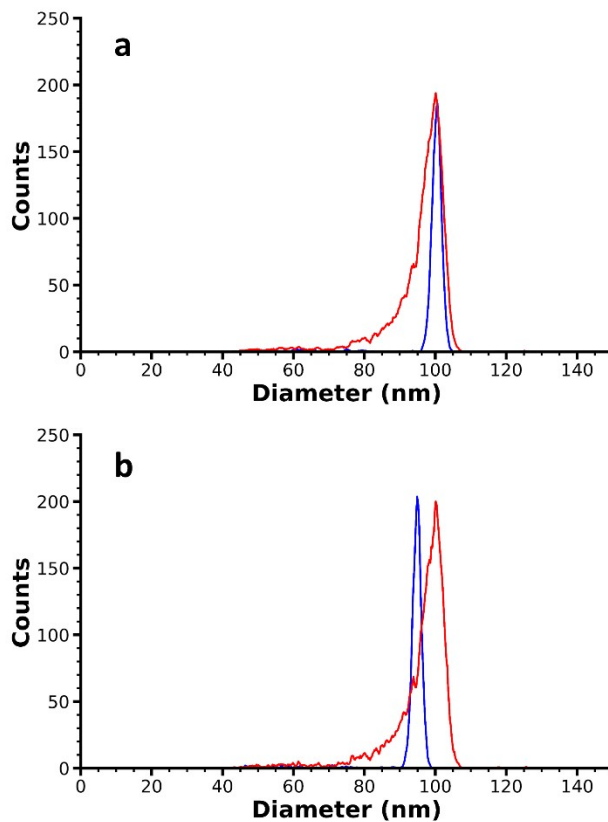
Figure 3. Diameter distributions produced from CDMS mass data for the CM nanoparticles (blue) and the Nanospheres (red). The data in (a) are based on densities estimated from bulk values whereas the data in (b) use densities determined directly from measured CDMS masses and TEM diameters. Both (a) and (b) assume a spherical nanoparticle geometry. While the bulk density estimate and measured density for the Nanospheres are similar and yield nearly identical distributions, the measured CM nanoparticle density is significantly higher than predicted from estimates of bulk values of the materials used in the synthesis processes and yields smaller diameters.
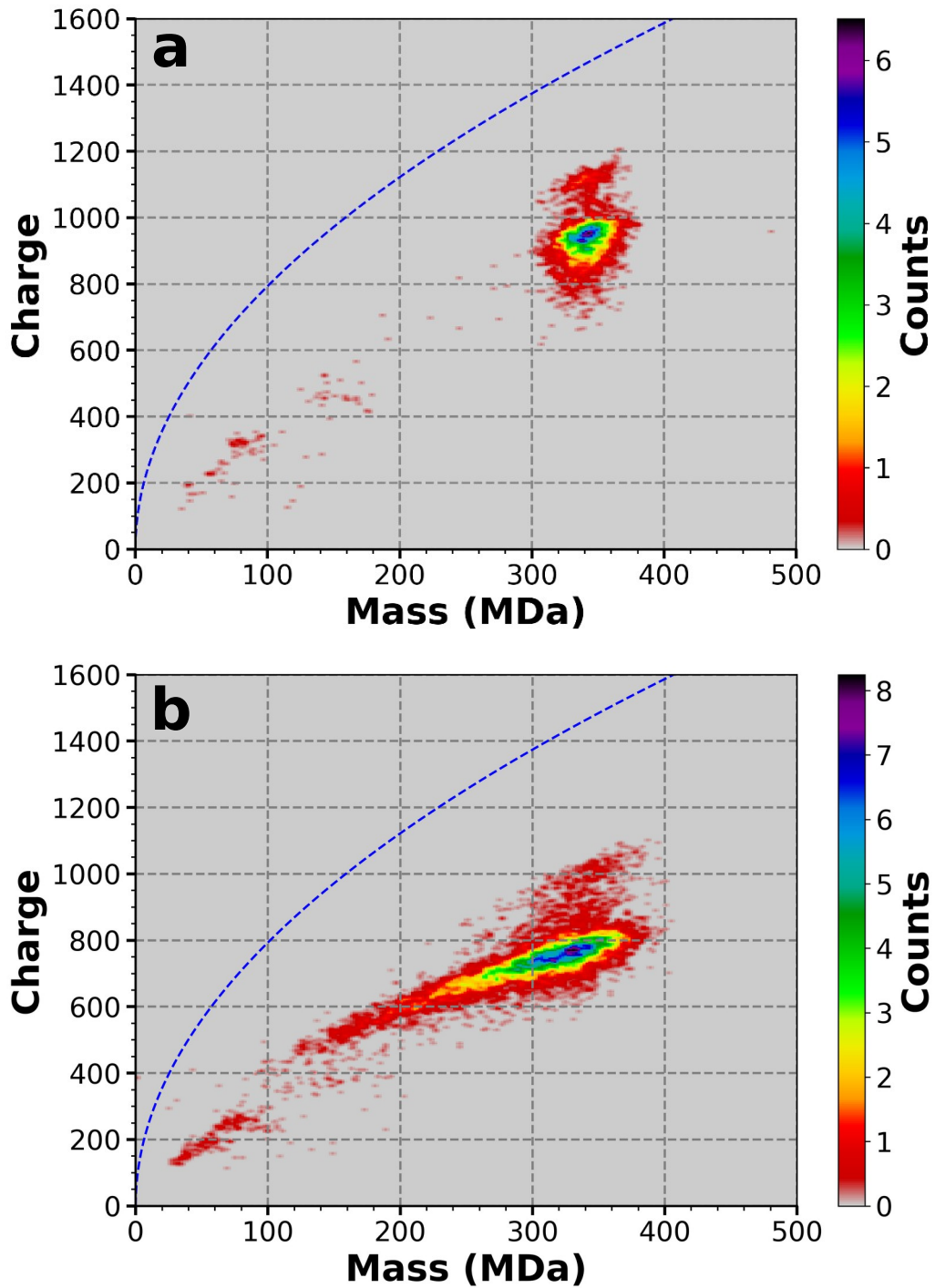
Figure 4. Two-dimensional mass vs. charge histograms for CM nanoparticles (a) and

Nanospheres (b). CM nanoparticles have a much higher average charge state (949 *e*) at peak

mass compared to the Nanospheres (772 e) despite their smaller measured diameters, indicating that the extent of charging is sensitive to the different surface composition of these two nanoparticle types. The blue dashed line describes the Rayleigh charge limit for a spherical water droplet of given mass.
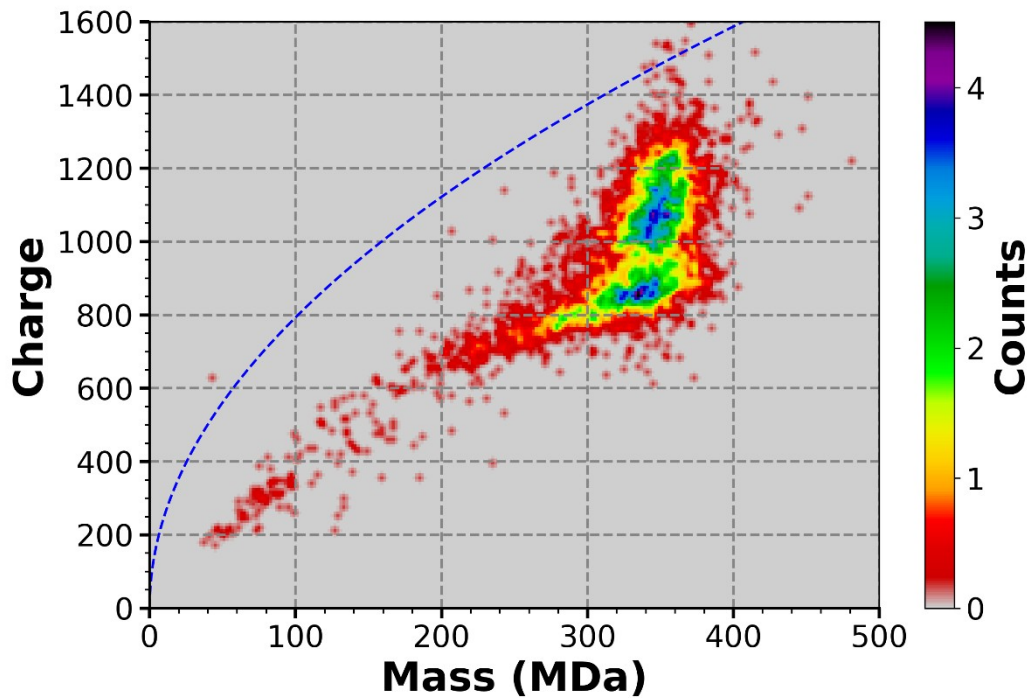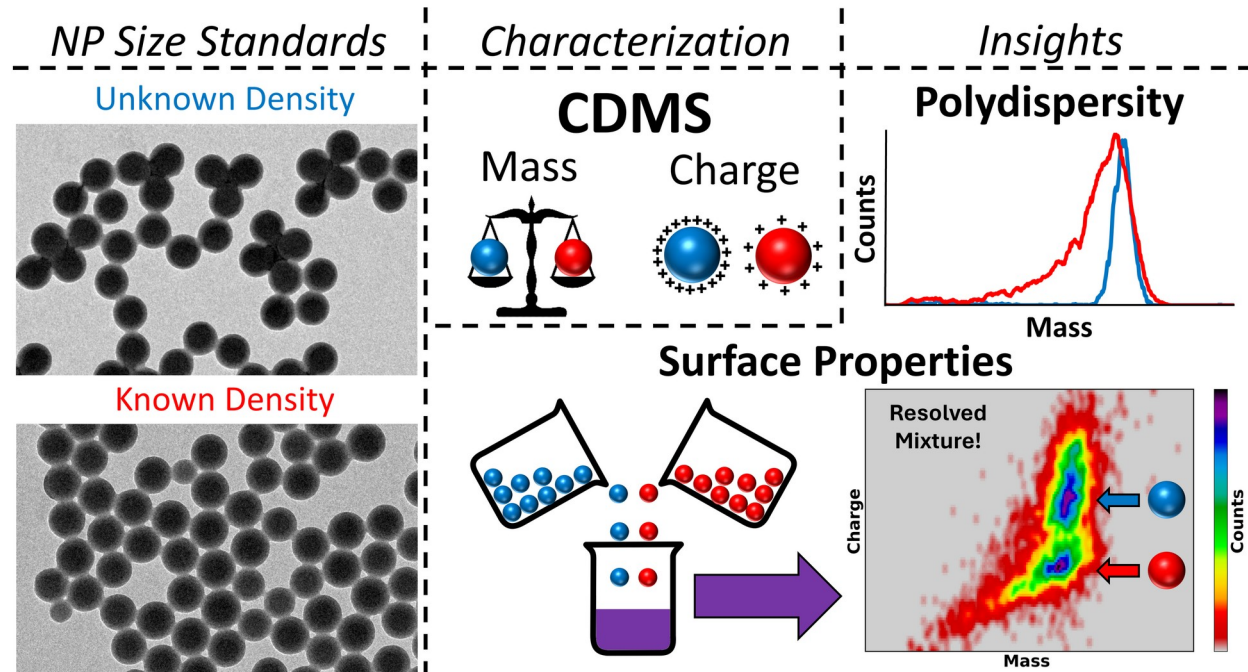
Figure 5. Two-dimensional mass vs. charge histogram produced from CDMS analysis of an approximately equimolar mixture of CM nanoparticles and Nanospheres. Two populations are well resolved by different extents of charging, with the lower charge distribution clearly identifiable as the Nanospheres by the characteristic tailing toward lower mass and charge also observed in Figure 4B.

For Table of Contents Only